International Journal of Thermophysics, Vol. 25, No. 5, September 2004 (© 2004)

Surface Adsorption and Orientation Near the Critical Point of Binary Liquid Mixtures[1]

J.-H. J. Cho,[2,3] B. M. Law,[2] and J. H. Carpenter[4]

Critical binary liquid mixtures have proven to be extremely useful for quantitatively studying wetting and adsorption phenomena that occur at the surfaces of these systems. In this paper recent experimental developments in our understanding of adsorption gained via the study of critical mixtures are reviewed. At the noncritical liquid/vapor surface the component possessing the smallest surface tension completely saturates this surface for sufficiently large surface tension differences $\Delta\sigma$ between the two components. This complete (or strong) adsorption is described by a universal scaling function P which depends upon the dimensionless depth z/ξ where ξ is the correlation length. Weakly polar and nonpolar binary liquid mixtures have been used to define the scaling function P. If the surface energy difference $\Delta\sigma$ between the two components is small, then the surface is no longer completely saturated by one component. In this weak adsorption regime the adsorption behavior is now described by a universal function G of both z/ξ and $\Delta\sigma$. The functional dependence of G is elucidated by examining a homologous series of critical binary AB liquid mixtures where component A is an n-alkane while component B (methyl formate) is fixed. For this system $\Delta\sigma$ changes sign with increasing n-alkane chain length. In addition to adsorption, dipole surface orientational order at the liquid/vapor surface of highly polar + nonpolar mixtures is also discussed. This orientational order is induced by the dipole-image dipole interaction in the vicinity of a surface.

KEY WORDS: adsorption; critical phenomena; ellipsometry; surface orientation.

[1]Paper presented at the Fifteenth Symposium on Thermophysical Properties, June 22–27, Boulder, Colorado, U.S.A.

[2]Department of Physics, Condensed Matter Physics Laboratory, Kansas State University, Manhattan, Kansas 66506-2601, U.S.A.

[3]To whom correspondence should be addressed. E-mail: jcho@phys.ksu.edu

[4]Department of Physics, University of Illinois at Urbana-Champaign, 1110 West Green Street, Urbana, Illinois 61801, U.S.A.

0195-928X/04/0900-1449/0

1. INTRODUCTION

Since Fisher and de Gennes [1] predicted the existence of preferential adsorption in critical binary liquid mixtures more than two decades ago, numerous theoretical [2–9] and experimental studies [10–19] have attempted to determine the surface universal behavior of these systems. However, it has only been in the last few years that a number of universal functions have been determined which are consistent with experimental results. The universal behavior is far more complex and interesting than had been supposed in the past; the local composition and local orientational order are found to depend upon the depth, surface energy, and dipole moment of the two components. The purpose of this paper is to briefly review our recent studies of critical adsorption phenomena [16–19].

2. CRITICAL ADSORPTION

At the surfaces of mixtures, the component with the lowest surface tension preferentially adsorbs at this interface. If this mixture happens to be near a critical point, then this phenomenon is called critical adsorption [1]. The surface composition therefore necessarily differs from the bulk composition; hence, for an AB critical binary liquid mixture, the local volume fraction $\nu_A(z)$ of the preferentially adsorbed component (assumed to be A) must depend upon the depth z away from the interface. A key length scale in critical systems is the correlation length,

$$\xi = \xi_o t^{-\nu}; \tag{1}$$

this quantity provides a measure of the bulk composition fluctuations as well as the characteristic thickness of the adsorption layer. Here ξ_o (~ 0.2 nm) is a system-dependent amplitude, ν ($=0.632$ [20]) is a universal critical exponent, and $t = |T - T_c|/T_c$ is the reduced temperature measured relative to the critical temperature T_c. The thickness of the adsorption profile therefore varies from ~ 0.5 nm at 30°C from T_c to ~ 300 nm within a few mK of T_c. This divergent behavior for $\nu_A(z)$ can be expressed as a universal function of the dimensionless depth z/ξ.

Critical phenomena are normally expressed in terms of an order parameter which, for critical binary liquid mixtures, corresponds to deviations of the volume fraction from the critical volume fraction ν_c, i.e., $m = \nu_A - \nu_c$ [21]. This order parameter,

$$\begin{aligned} m &= 0 && \text{in the one-phase region} \\ &= M_- t^{\beta} && \text{in the two-phase region,} \end{aligned} \tag{2}$$

provides a measure of the bulk concentration where M_- is a system dependent parameter while the exponent β ($= 0.328$ [20]) is a universal critical exponent. A corresponding *surface order parameter*, defined as $m(z) = \nu_A(z) - \nu_c$, describes how the surface composition deviates from the critical value ν_c. The remainder of this paper provides a discussion of $m(z)$.

As discussed above, $m(z)$ must be a function of the dimensionless depth z/ξ. It must also be a function of other parameters. In particular, $m(z)$ must be a function of a surface field h_1 [6] which is proportional to the difference in surface energies between the two components ($\sigma_A - \sigma_B$). This functional variation is normally expressed in the following manner [9]:

$$m(z) = M_- t^{\beta} G(x, y) \tag{3}$$

where $G(x, y)$ is a universal scaling function, $x = (z + z_e)/\xi$, $y = h_1 t^{-\Delta_1}$, Δ_1 ($= 0.461$ [9]) is a surface exponent, and z_e is a system-dependent extrapolation length [16]. The aim of this field is to determine the universal function $G(x, y)$ which describes experimental critical adsorption data. Once $G(x, y)$ has been determined, then critical adsorption for any other system can be predicted once a few system-dependent parameters (ξ_o, M_-, ν_c, h_1) have been measured.

This complicated problem simplifies in the strong field limit $|h_1| \gg 0$ when the surface is completely saturated with the component possessing the lowest surface energy, a situation called strong adsorption. In this saturation limit, $G(x, y)$ becomes independent of the precise value for y and reduces to a function of the single variable x, namely, $G(x, y) \to P(x)$ as $y \to \infty$ [6, 18]. If, however, $h_1 \approx 0$ (termed weak adsorption), neither component dominates the surface composition and both variables x and y which appear in $G(x, y)$ are important. In Fig. 1, we compare strong adsorption with weak adsorption via their representative universal functions, P and G, respectively. In the strong surface energy limit the local volume fraction at the surface is saturated at its maximum value, $\nu_A(z = 0) = 1$. By comparison, for weak adsorption the local volume fraction at the surface is proportional to the surface field h_1 where the influence of the surface field dominates the behavior close to the surface, within $z \leqslant |h_1|^{-\nu/\Delta_1}$ (Fig. 1). Far from the surface ($z \gg |h_1|^{-\nu/\Delta_1}$), both scaling functions, $G(x, y)$ and $P(x)$, become indistinguishable.

Various theoretical methods including Monte Carlo simulations [4], surface renormalization group theory [3], and local functional theory [8] have become available for describing strong adsorption; however, these theories only provide a qualitative description of experiments [16]. The

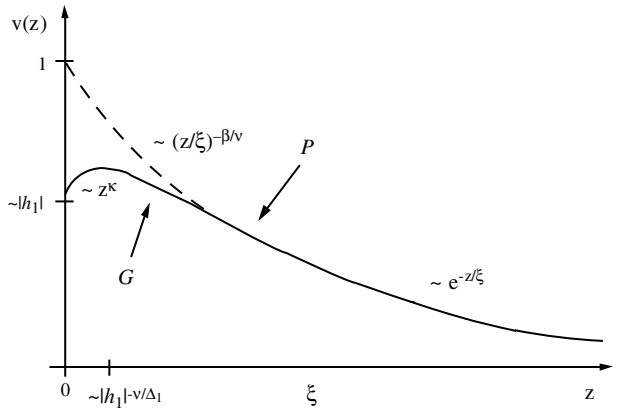

Fig. 1. Schematic diagram of strong P (dashed line) and weak G (solid line) adsorption as a function of depth. The exponent $\kappa = (\Delta_1 - \beta)/\nu \approx 0.21$.

universal functions P and G that we have determined from experiments are discussed below.

2.1. Strong Adsorption

In the strong surface field limit ($|h_1| \gg 0$) where the surface is occupied predominantly by the component with the smaller surface tension, the interfacial structure is given by

$$m(z) = M_- t^{\beta} P(x) \tag{4}$$

according to Eq. (3) [1]. The universal function P for the strong adsorption of a number of different weakly polar [16] + nonpolar [17] critical mixtures has been determined by using the optical reflection technique of ellipsometry. In the analysis of these experiments, the leading order terms predicted by theory [2, 3] at small and large x were retained where the coefficients were estimated from data [16]. The results can be summarized as follows:

$$P_<(x) = \begin{pmatrix} 0.788 \\ 1.117 \end{pmatrix} x^{-\beta/\nu} + \begin{pmatrix} -0.245 \\ 0.169 \end{pmatrix} x^{(1-\beta)\nu} \quad \text{for } x \leqslant 1.15, \text{ and}$$

$$P_>(x) = \begin{pmatrix} 0 \\ 1 \end{pmatrix} + \begin{pmatrix} 0.963 \\ 0.572 \end{pmatrix} e^{-x} + \begin{pmatrix} 1.437 \\ 0.533 \end{pmatrix} e^{-2x} \quad \text{for } x \geqslant 1.15, \tag{5}$$

where $P_<(P_>)$ describes the small (large) x region while the upper (lower) row describes the one- (two-) phase region of the liquid mixture. This

particular construction of the $P(x)$ function is continuous at T_c, possesses the predicted functional dependencies at small and large x, while at the same time being continuous in value and slope for all x. A comparison between Eq. (5) (dashed lines) and experimental ellipticity data $\bar{\rho}$ (open symbols) in the one-phase region for four mixtures is shown in Fig. 2a where the ellipticity $\bar{\rho} = \mathrm{Im}(r_p/r_s)|_{\theta_B}$ at the Brewster angle θ_B with r_i the complex reflection amplitude for polarization i [22, 23].

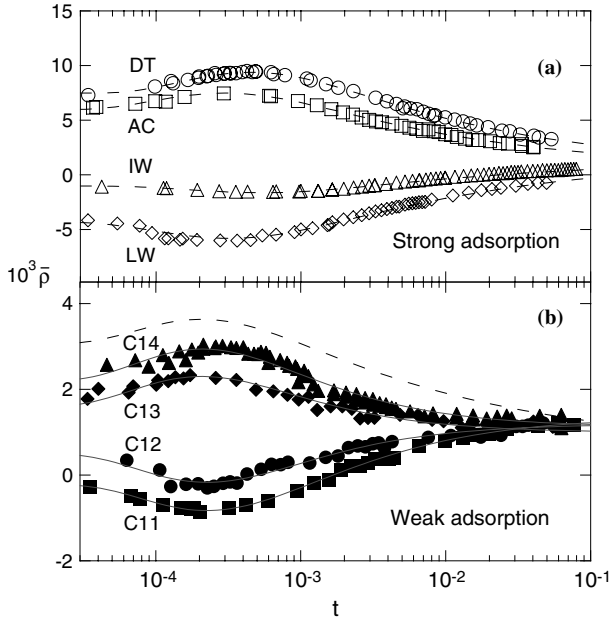

Fig. 2. One-phase strong and weak adsorption. (a) Strong adsorption for dodecane + tetrabromoethane (DT) [15], aniline + cyclohexane (AC), isobutyric acid + water (IW), and 2,6-lutidine + water (LW) [16] which is well described by the P function (dashed lines) where the surface field $|h_1| \gg 0$. (b) Weak adsorption ($h_1 \approx 0$) for the homologous series of mixtures, methyl formate + n-alkane [18] which is well described by the G function (Eqs. (6) and (7), solid lines). The dashed line represents the strong adsorption prediction (P function) for $h_1 \gg 0$. Note: in this figure the variations for the different mixtures are mainly caused by differing optical dielectric constants in (a) and differing surface fields h_1 in (b).

2.2. Weak Adsorption

The P function, which describes strong adsorption, is only applicable when $|h_1| \gg 0$. For arbitrary values of h_1, and in particular for weak adsorption where $h_1 \approx 0$, the G function (Eq. (3)) must be used [6]. This function can be re-expressed as [18]

$$G(x, y) = P(x)Z(x, y) \tag{6}$$

where Z provides a measure of how G deviates from P.

The G function has been studied by systematically changing the second variable y, using a homologous series of critical mixtures [18]. Here component B (= methyl formate) is fixed while component A is varied by considering the n-alkanes from n-undecane (denoted C11) to n-tetradecane (C14). For this homologous series of critical mixtures, h_1 varies continuously from a negative to positive value with increasing n-alkane chain length where $h_1 = 0$ occurs at a value of C12.6. A model for the crossover function Z,

$$Z(x, y) = (1 - e^{-\varsigma})^{\Delta_1/\nu} \tag{7}$$

based on theory [6], provides an excellent description of ellipsometric data in the one-phase region where $\varsigma \sim x\,|y|^{\nu/\Delta_1}$. In the two-phase region, the crossover function has also been determined, but is more complicated [18]. The solid lines in Fig. 2b compare Eq. (7) with experimental ellipticity data (solid symbols) for weak adsorption. Significant departure is found between the weak adsorption data and the strong adsorption P behavior of Eq. (5) indicated by the dashed line in Fig. 2b.

For the mixture methyl formate + C13 or C14 a wetting layer of the heavier methyl formate rich phase forms at the liquid/vapor surface in the two-phase region of this liquid mixture. In the insets of Fig. 3 we show the time dependence of the ellipticity $\bar{\rho}$ for three different reduced temperatures after a temperature quench from the one-phase into the two-phase region. Rather complex behavior is observed. Initially a metastable state forms soon after the temperature quench. This metastable state, indicated by the open triangles in Fig. 3, agrees with the behavior predicted for weak adsorption (solid line) [18]. The time variation of $\bar{\rho}$ (which depends upon the temperature quench depth) is not well understood. At late times (of order $\sim$1 day) an equilibrium wetting layer of thickness L is attained. In other work [24], we have shown that L diverges *continuously* on approaching a wetting temperature T_w where this divergence is well described by a modified mean-field short-ranged critical wetting transition.

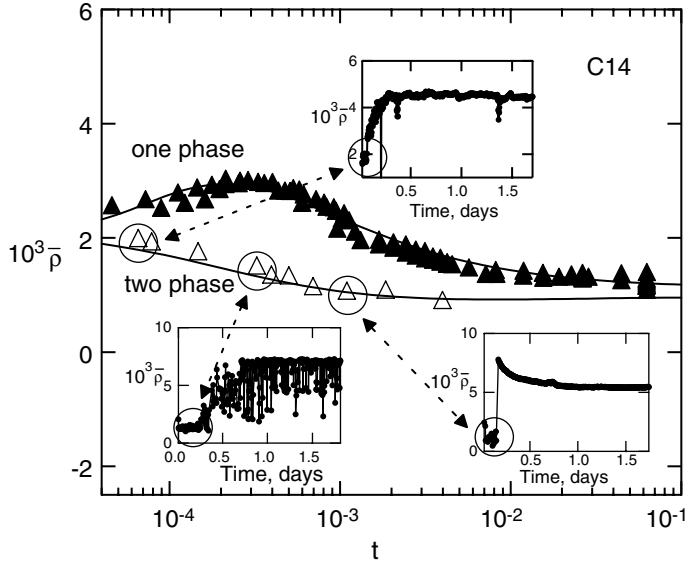

Fig. 3. Weak adsorption in the one- and two-phase regions for the methyl formate + tetradecane (C14) mixture. The calculated curves (Eqs. (6) and (7)) fit the $\bar{\rho}$ data well in both the one- (solid symbols) and two-phase (open symbols) regions. For the two-phase region, the adsorption data were obtained by averaging the metastable data (circled regions in the insets). The metastable adsorption lasts a few hours or less, depending upon the reduced temperature t. The insets depict the time dependent $\bar{\rho}$ data at three different temperatures after a temperature quench from the one-phase into the two-phase regime.

3. SURFACE ORIENTATION OF HIGHLY POLAR LIQUIDS

In addition to preferential adsorption, if one (or both) component(s) of the mixture is highly polar, then this polar component may align in a particular direction when in the vicinity of a boundary due to its interaction with its image dipole. It has been well-documented via both theory [25] and experiment [26] that this dipole-image dipole interaction causes surface orientational order at the *critical* liquid/liquid interface of highly polar + nonpolar binary liquid mixtures.

At the *noncritical* liquid/vapor interface of critical binary liquid mixtures, the surface dipolar orientational order has rather a different character than found previously at the *critical* liquid/liquid interface. This dipole-image dipole effect at noncritical interfaces is described in this section. For a nonpolar (A) + highly polar (B) critical mixture with surface tension difference, $\Delta\sigma = \sigma_A - \sigma_B \ll 0$, one is in the strong

adsorption regime where component A completely saturates the surface. However, there is a dipole-image dipole interaction for component B where the energy of this interaction is given by [25, 27]

$$U = p^2 \frac{(\varepsilon_\alpha - \varepsilon_v)(1+\cos^2\theta)}{(\varepsilon_\alpha + \varepsilon_v)d^3} \tag{8}$$

with d the distance between the dipole and its image, θ the angle between the dipole direction and the surface normal (Fig. 4, inset) while $\varepsilon_v(\varepsilon_\alpha)$ is the static dielectric constant of the vapor (liquid). Of course, at a liquid/vapor surface $\varepsilon_\alpha > \varepsilon_v$ and this energy is minimized for $\theta = \pi/2$ or $3\pi/2$ and the dipoles prefer to orient parallel to the interface where in addition the dipoles tend to be repelled from the interface because U is positive.

This electrostatic model only provides a qualitative picture of the dipole-induced orientational order. In practice, the situation is far more complicated because the liquid/vapor interface is never sharp but instead possesses a thickness ξ over which the local volume fraction also varies with position. The local volume fraction of dipolar molecules with orientation θ at position z can be written as [25]

$$\nu_B(z,\theta) \sim \nu_B(z)[1+\alpha_2(z)(3\cos^2\theta - 1)] \tag{9}$$

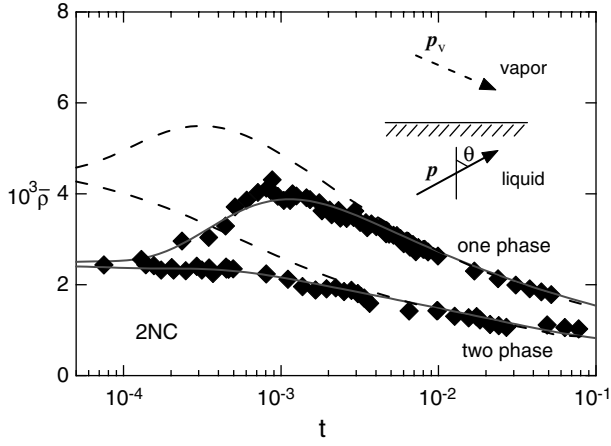

Fig. 4. Strong adsorption in the presence of dipole orientational order, for the highly polar mixture 2-nitroanisole + cyclohexane [18]. Our model (Eq. (10), solid line) is in agreement with the $\bar{\rho}$ data (symbols). The dashed line represents the predicted dependency in the absence of orientational order (Eq. (5)). The inset depicts a dipole (solid arrow) interacting with its image dipole (dashed arrow) in the vicinity of an interface.

in the absence of any external field. Here, the position dependent parameter $\alpha_2(z)$ describes the variation in orientational order with depth.

In a recent series of experiments [19], we have studied the nonpolar + highly polar mixtures, cyclohexane + 2-nitroanisole (Fig. 4, solid diamonds) and cyclohexane + 4-nitroanisole, where the highly polar nitroanisole desorbs from the surface because it possesses a high surface tension, but also orients parallel to the interface due to its interaction with its image dipole. Since no theoretical prediction for $\alpha_2(z)$ at the noncritical interface is currently available, a general scaling expression, $\alpha_2(z) \sim t^{\phi} Y(x)$, has been used to fit our ellipsometric data. The exponent ϕ is an adjustable parameter, and $Y(x)$ is a universal function of the dipole orientational order. The optimal description of experimental data indicates that $\phi \sim 2\beta$ and $Y(x) \sim P(x)^2$. Thus, the orientational order can be expressed by a simple form,

$$\alpha_2(z) \sim [m(z)]^2. \tag{10}$$

The ellipticity calculated for this anisotropic interface is shown in Fig. 4 (solid line), which differs significantly from the behavior predicted in the absence of any orientational order where $\alpha_2(z) = 0$ (dashed line).

4. SUMMARY

Surface adsorption at the liquid/vapor interface of critical binary liquid mixtures depends upon the dimensionless depth z/ξ, surface energy difference $\Delta\sigma$, and polarity p of the two components. For weakly polar or nonpolar mixtures, in the limit of strong adsorption ($|\Delta\sigma| \gg 0$) where one component completely saturates the surface, the local volume fraction can be described by a universal surface scaling function P which is solely a function of z/ξ. We have determined an estimate for the P function (Eq. (5)) from experimental ellipsometric data that provides a good description of the adsorption behavior for a number of different critical liquid mixtures (Fig. 2a). If the surface energy difference $|\Delta\sigma| \leqslant 6\,\mathrm{mJ \cdot m^{-2}}$, then the surface is no longer dominated by a single component and the adsorption behavior must be described by a more generalized surface scaling function G which is a function of both z/ξ and $\Delta\sigma$. In this weak adsorption situation we have estimated the G function using a homologous series of n-alkane + methyl formate mixtures where the surface tension difference $\Delta\sigma$ is relatively small and varies from a negative to positive value with increasing n-alkane chain length. The functional form for G (Eqs. (6) and (7)) provides an excellent description of experimental ellipsometric data (Fig. 2b).

For nonpolar + highly polar mixtures the adsorption profile is no longer isotropic and one must consider the interfacial orientation of the polar component in addition to the adsorption. For critical mixtures, where the polar component is desorbed from the liquid/vapor interface, we have determined that the surface orientational order is proportional to the square of the local volume fraction order parameter (Eq. (10)). The long-ranged dipole—image dipole repulsion stretches the adsorption profile (i.e., $\xi_o > \xi_o$ (*bulk*) [19]) where the dipoles prefer to orient parallel to the surface. These observations are still not fully understood but are consistent with simple electrostatic considerations.

In summary, by systematically controlling the physical variables of a number of critical AB liquid mixtures, we have examined critical adsorption and surface orientational order that are prevalent at the noncritical liquid/vapor surface of these mixtures. Although the technique of ellipsometry provides high depth resolution, other techniques such as X-ray or neutron reflectometry must be employed in order to fully verify the universal functions that we have determined. An understanding of these fundamental scientific issues will have important implications on various related fields, such as surface physics, chemistry, biology, etc.

ACKNOWLEDGMENTS

This research work was supported by the Donors of the Petroleum Research Fund, administrated by the American Chemical Society, and by the U.S. National Science Foundation, most recently through Grant No. DMR-0097119.

REFERENCES

1. M. E. Fisher, P. G. de Gennes, and C. R. Seances, *Acad. Sci. Ser. B* **287**:207 (1978).
2. A. J. Liu and M. E. Fisher, *Phys. Rev. A* **40**:7202 (1989).
3. H. W. Diehl and M. Smock, *Phys. Rev. B* **47**:5841 (1993), **48**:6470(E) (1993).
4. M. Smock, H. W. Diehl, and D. P. Landau, *Ber. Bunsen. Phys. Chem*. **98**:486 (1994).
5. G. Flöter and S. Dietrich, *Z. Phys. B* **97**:213 (1995).
6. U. Ritschel and P. Czerner, *Phys. Rev. Lett*. **77**:3645 (1996), *Physica A* **237**:240 (1997).
7. S. B. Kiselev, J. F. Ely, and M. Yu. Belyakov, *J. Chem. Phys*. **112**:3370 (2000).
8. Z. Borjan and P. J. Upton, *Phys. Rev. E* **63**:065102 (2001).
9. H. W. Diehl, in *Phase Transition and Critical Phenomena*, C. Domb and J. L. Lebowitz, eds. (Academic, London, 1986), *Int. J. Mod. Phys. B* **11**:3503 (1997).
10. D. Beaglehole, *J. Chem. Phys*. **73**:3366 (1980).
11. C. Franck and S. E. Schnatterly, *Phys. Rev. Lett*. **48**:763 (1982).
12. B. Heidel and G. H. Findenegg, *J. Phys. Chem*. **88**:6575 (1984), *J. Chem. Phys*. **87**:706 (1987).
13. J. W. Schmidt and M. R. Moldover, *J. Chem. Phys*. **83**:1829 (1985).

14. D. Beaglehole, in *Fluid Interfacial Phenomena*, C. A. Croxton, ed. (Wiley, New York, 1986).
15. D. S. P. Smith, B. M. Law, M. Smock, and D. P. Landau, *Phys. Rev. E* **55**:620 (1997).
16. J. H. Carpenter, B. M. Law, and D. S. P. Smith, *Phys. Rev. E* **59**:5655 (1999), J. H. Capenter, J.-H. J. Cho, and B. M. Law, *Phys. Rev. E* **61**:532 (2000).
17. J.-H. J. Cho, B. M. Law, and K. Gray, *J. Chem. Phys*. **116**:3058 (2002).
18. J.-H. J. Cho and B. M. Law, *Phys. Rev. Lett*. **86**:2070 (2001), *Phys. Rev. E* **65**:011601 (2001).
19. J.-H. J. Cho and B. M. Law, *Phys. Rev. Lett*. **89**:146101 (2002), *Phys. Rev. E* **67**:031605 (2003).
20. M. E. Fisher and J.-H. Chen, *J. Phys. (Paris)* **46**:1645 (1985).
21. A. Kumar, H. R. Krishnamurthy, and E. S. R. Gopal, *Phys. Rep*. **98**:57 (1983).
22. D. Beaglehole, *Physica* (Amsterdam) *B* **100**:163 (1980).
23. The local volume fraction $\nu(z)$ is first converted to an optical dielectric profile $\varepsilon(z)$, using the Clausius-Mossotti equation (R. F. Kayser, *Phys. Rev. B* **34**:3254 (1986)). Maxwell's equations are then solved numerically for the reflection amplitudes r_i (B. M. Law and D. Beaglehole, *J. Phys. D* **14**:115 (1981)).
24. J.-H. J. Cho and B. M. Law, unpublished.
25. P. Frodl and S. Dietrich, *Phys. Rev. A* **45**:7730 (1992), *E* **48**:3741 (1993).
26. A. Mukhopadhyay and B. M. Law, *Phys. Rev. E* **63**:011507 (2000).
27. J. D. Jackson, *Classical Electrodynamics*, 2nd Ed. (Wiley, New York, 1993).